iScience

Article

Adipocyte Angptl8 deletion improves glucose and energy metabolism and obesity associated inflammation in mice

Graphical abstract

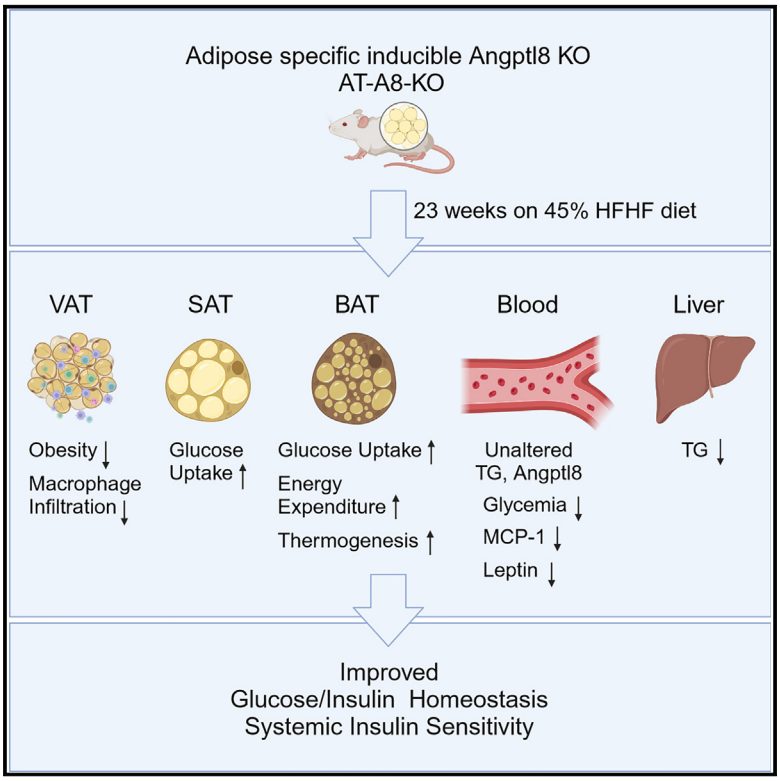

Highlights

- Angptl8 (A8) regulates LPL activity but the role of adipose A8 remains elusive
- Adipose-A8-KO (AAKO) mice on high fat/fructose diet (HFD) show lower BW and glycemia
- AAKO mice on HFD show higher early dark phase energy expenditure and reduced inflammation
- Adipose A8 plays a role in whole body glucose and energy homeostasis in obesity

Authors

Anindya Ghosh, Isabelle Chénier, Yat Hei Leung, ..., Fahd Al-Mulla, Marc Prentki, Mohamed Abu-Farha

Correspondence

marc.prentki@umontreal.ca (M.P.), mohamed.abufarha@dasmaninstitute.org (M.A.-F.)

In brief

Biochemical mechanism

Ghosh et al., 2024, iScience 27, 111292
December 20, 2024
https://doi.org/10.1016/j.isci.2024.111292

CellPress

iScience

CellPress
OPEN ACCESS

Article

Adipocyte Angptl8 deletion improves glucose and energy metabolism and obesity associated inflammation in mice

Anindya Ghosh,[1,4] Isabelle Chénier,[1,4] Yat Hei Leung,[1] Abel K. Oppong,[1] Marie-Line Peyot,[1] S. R. Murthy Madiraju,[1] Irina Al-Khairi,[2] Jehad Abubaker,[2] Fahd Al-Mulla,[3] Marc Prentki,[1,5,*] and Mohamed Abu-Farha[2,3,*]

[1]Departments of Nutrition, Biochemistry and Molecular Medicine, University of Montreal, and Montreal Diabetes Research Center, Centre de Recherche Du Centre Hospitalier de L'Université de Montréal (CRCHUM), Montréal, QC, Canada
[2]Biochemistry and Molecular Biology Department, Dasman Diabetes Institute, Dasman 15462, Kuwait
[3]Translational Research Department, Dasman Diabetes Institute, Dasman 15462, Kuwait
[4]These authors contributed equally
[5]Lead contact
*Correspondence: marc.prentki@umontreal.ca (M.P.), mohamed.abufarha@dasmaninstitute.org (M.A.-F.)
https://doi.org/10.1016/j.isci.2024.111292

SUMMARY

Angiopoietin-like protein 8 (Angptl8), expressed in the liver and adipocytes, forms a complex with Angptl3 or Angptl4, which regulates lipoprotein lipase and triglyceride metabolism. However, the precise functions of adipocyte Angptl8 remain elusive. Here we report that adipocyte-specific inducible Angptl8-knockout (AT-A8-KO) male mice on normal diet showed minor phenotypic changes, but after a high-fat high fructose (HFHF) diet, exhibited decreased body weight gain and glycemia, elevated rectal temperature and early dark phase energy expenditure compared to the Cre controls. AT-A8-KO mice also displayed improved glucose tolerance, a trend for better insulin sensitivity, improved insulin-stimulated glucose uptake in adipose tissues, and reduced visceral adipose tissue crown-like structures, plasma MCP-1 and leptin levels. The results indicate the importance of adipose Angptl8 in the context of nutri-stress and obesity, as its deletion in mice promotes a metabolically healthy obese phenotype by slightly ameliorating obesity, improving glucose and energy homeostasis, and mitigating inflammation.

INTRODUCTION

Adipose tissue is the primary energy reservoir in vertebrates, as it stores energy in the form of triglycerides (TG) generated via *de novo* lipogenesis (DNL) during feeding, and releases free fatty acids (FFA) by lipolysis in bloodstream during fasting, to be utilized by other tissues.[1] Feeding is known to induce the expression of lipogenic enzymes and the corresponding transcription factors (SREBP-1c, LXRα and USF) that are involved in *de novo* lipogenesis as well as lipogenesis (fat esterification) in rodents.[2] Circulating TGs are hydrolyzed by lipoprotein lipase (LPL), located on the capillary endothelium, to generate FFAs, which are taken up by adjacent tissues.[3] The differential activity of LPL in various tissues plays a key role in partitioning circulating TGs between oxidative tissues (heart, muscle, brown adipose) and white adipose tissues (WAT).[4,5] In fed mice, LPL activity is suppressed in oxidative tissues while increased in WAT, channeling circulating FFAs toward storage in WAT.[6,7] Conversely, in the fasted state, LPL activity in oxidative tissues increases while decreasing in WAT, promoting the uptake and oxidation of FFA in the oxidative tissues.[4,8]

The activity of LPL is regulated in a tissue specific manner through its interactions with apolipoproteins and three members of the angiopoietin-like protein (ANGPTL) family – ANGPTL3 (A3), ANGPTL4 (A4) and ANGPTL8 (A8) that are secreted into circulation.[8,9] Structurally, A3 and A4 share similarities, featuring an *N*-terminal coiled-coil domain that contains the LPL interaction site and relevant for LPL inhibition and a C-terminal fibrinogen-like domain. In contrast, A8 lacks the C-terminal fibrinogen-like domain.[10] The roles of A3 and A4 in LPL inhibition and TG metabolism are well established and genetic inactivation of A3 or A4 has been shown to reduce serum TG in both mice and humans.[8,9,11–14] A8, also known as RIFL, Lipasin or betatrophin, is predominantly expressed in hepatocytes and adipocytes, and is regulated by nutritional cues.[15] Thus, during fasting, A8 expression is decreased whereas feeding stimulates its expression in both hepatocytes and adipocytes.[10,16,17] Circulating A8 exerts dual action on LPL activity depending on its interaction with A3 or A4.[18,19] LPL activity is inhibited by the complex formed by A8 and A3 [18–20]. Conversely, the inhibitory effect of A4 on LPL activity is alleviated by A8 by forming a complex with A4, and this becomes particularly relevant in WAT depots during fasting, when the expression of A8 is much reduced while that of A4 is elevated.[7,18,21–24] Thus, the complex of A8 and A3 is inhibitory to LPL as noticed in A3$^{-/-}$ mice,[10] while A8 alleviates the inhibitory effect of A4 on LPL activity by forming a complex with A4,

and this is particularly relevant in WAT depots during fasting.[25] This dual effect of A8 on LPL underlies its ability to coordinate TG partitioning between oxidative tissues and WAT.[7,10,26,27] Indeed, the significance of A8 in the control of TG metabolism became evident in studies showing a ~5-fold increase in plasma TG levels following A8 overexpression in the livers of mice,[10,16] whereas mice with global deletion of A8 exhibited reduced body weight gain and fat mass, and a 2-fold reduction in plasma TG levels.[28] Moreover, $A8^{-/-}$ male mice on C57BL/6J background exhibited increased oxygen consumption, rectal temperature under fed conditions at room temperature and following cold exposure.[29] These phenotypes were found to be more prominent in $A3^{-/-}$ $A8^{-/-}$ double KO mice.[30]

In addition to the regulation of LPL activity by the circulating A8, increasing evidence suggests that A8 may also have intracellular and plasma membrane receptor mediated functions that are relevant for controlling adipogenesis,[17,30] NF-κB mediated inflammation and autophagy,[31,32] intracellular lipolysis[33] and the circadian clock.[34,35] The significance of circulating A8 in health and disease became evident from the several studies showing association of elevated plasma A8 levels with various metabolic disorders including type 2 diabetes, arteriosclerosis, dyslipidemia and non-alcoholic steatohepatitis (NASH).[35–38]

A recent report using constitutive whole-body $A8^{-/-}$, and the conditional (embryonic; not inducible) liver-specific (Ls-$A8^{-/-}$), and adipocyte-specific (As-$A8^{-/-}$) A8 KO mice on the C57BL/6N background revealed distinct functions of liver and adipocyte-derived A8.[7] It was shown that liver is the major source of circulating A8, and in the fed state A8 forms a complex with A3 in the hepatocytes, which is then secreted into circulation to inhibit LPL in oxidative tissues in an endocrine manner.[7] Moreover, as noticed with the whole body A8 deleted mice,[7] liver specific deletion of A8 in mice leads to diminished plasma TG levels and elevated intravascular LPL activity in the fed state. However, in the WAT, A8 produced by adipocytes plays a distinct role locally by forming a complex with A4 and targeting A4 for degradation, thereby releasing LPL from A4 inhibition.[7] Additionally, adipocyte-specific deletion of A8 in mice fed a normal diet was found to increase plasma TG, rectal temperature in the fed condition without affecting intravascular LPL activity and to induce WAT browning, emphasizing the distinct autocrine/paracrine effects of adipose A8.[7] Thus, A8 arising from liver and adipose tissues regulates TG clearance and metabolism according to nutritional state.[7,18–20,39] However, the role of adipose A8 in whole-body glucose homeostasis, lipid metabolism, inflammation, cold-induced thermogenic programming, particularly under the obesity condition remains unknown.

Even though the earlier studies employing conditional (embryonic; not inducible) adipose A8 knockout mice revealed some role of A8 in adipose metabolism, the possibility that the deletion of A8 from the embryonic stage may have confounding effects on adipose development has not been addressed.[7] In the present study, we generated tamoxifen-inducible adipose-specific A8 knockout (AT-A8 KO) mice on C57BL/6N genetic background to investigate how deletion of adipose A8 in adult mice influences diet-induced obesity and energy expenditure, thereby avoiding any unwanted effects on adipose tissue during development. We noticed that AT-A8 KO mice fed a high-fat-high-fructose (HFHF) diet for 23 weeks, gained less body weight and exhibited improved glucose tolerance and insulin sensitivity and reduced insulinemia and inflammation compared to controls, indicating that adipose A8 plays a role in whole body glucose and insulin homeostasis as well as the response to diet induced obesity.

RESULTS

Mature adipocyte specific deletion of ANGPTL8

We examined the significance of adipocyte specific A8 in the regulation of insulin and energy homeostasis using tamoxifen inducible, adipose-specific A8 knockout (AT-A8-KO) mice on the C57BL/6N genetic background. Unlike the adipose A8-deleted (from embryonic stage) mice employed in an earlier study,[7] the inducible AT-A8-KO mice used here cannot suffer from any potential developmental effects as A8 is deleted in mature adipocytes of adult mice. Eight-week-old male Angptl8fl/fl-Cre+ mice received TMX via oral gavage to induce deletion of A8 in mature adipocytes. The littermate Cre mice were chosen as controls as they receive TMX oral gavage and express the Cre recombinase transgene, unlike the Fl/Fl and WT mice, to avoid potential effects by TMX and Cre recombinase on the phenotype. Additionally, given the similar phenotypes of WT and Fl/Fl mice (Figures S1A–S1H), Cre mice were used as the control group for all experiments.

Three to five weeks after TMX administration (11–13 weeks of age), A8 deletion was assessed by measuring mRNA levels in the three different fat tissues (VAT, SAT, and BAT) and also in the liver of mice fed a normal diet. A8 expression was markedly decreased in the AT-A8-KO mice compared to Cre mice in all the three fat depots, while it remained unchanged in the liver (Figure 1C). A8 protein levels were also significantly lowered in the mature adipocytes from VAT and SAT of the normal diet fed AT-A8-KO mice (Figure 1D) and also HFHF fed AT-A8-KO mice (Figures S2A and S2B) compared to the adipocytes from corresponding control Cre mice. There were no differences in body weight (Figure 1E), lean and fat mass (Figure 1F) or fasting glycemia (Figure 1G) between the Cre and KO mice on a normal diet.

AT-A8-KO mice on HFHF diet exhibit reduced body weight gain and glycemia but elevated rectal temperature and energy expenditure during feeding

AT-A8-KO mice and the Cre controls were fed either a control diet (ND) or high fat diet (45% kcal fat) supplemented with 30% fructose in water (HFHF) for 23 weeks (Figure 2A).[40] Both AT-A8-KO and Cre mice on HFHF diet exhibited body weight gain, increased total caloric intake and total fat mass compared to the corresponding normal diet fed mice (Figure 2B–2D). Although AT-A8-KO and Cre mice showed similar body weight gain on normal diet, AT-A8-KO mice fed HFHF diet gained less weight than the Cre mice controls on the same diet (Figure 2B). Caloric intake, percentage fat and lean mass did not differ among the groups on either diet (Figures 2C–2E). Furthermore, HFHF diet feeding led to elevated fasting glycemia in the Cre mice compared to the control diet fed Cre mice. However, compared to normal diet, HFHF diet had no effect on the fasting

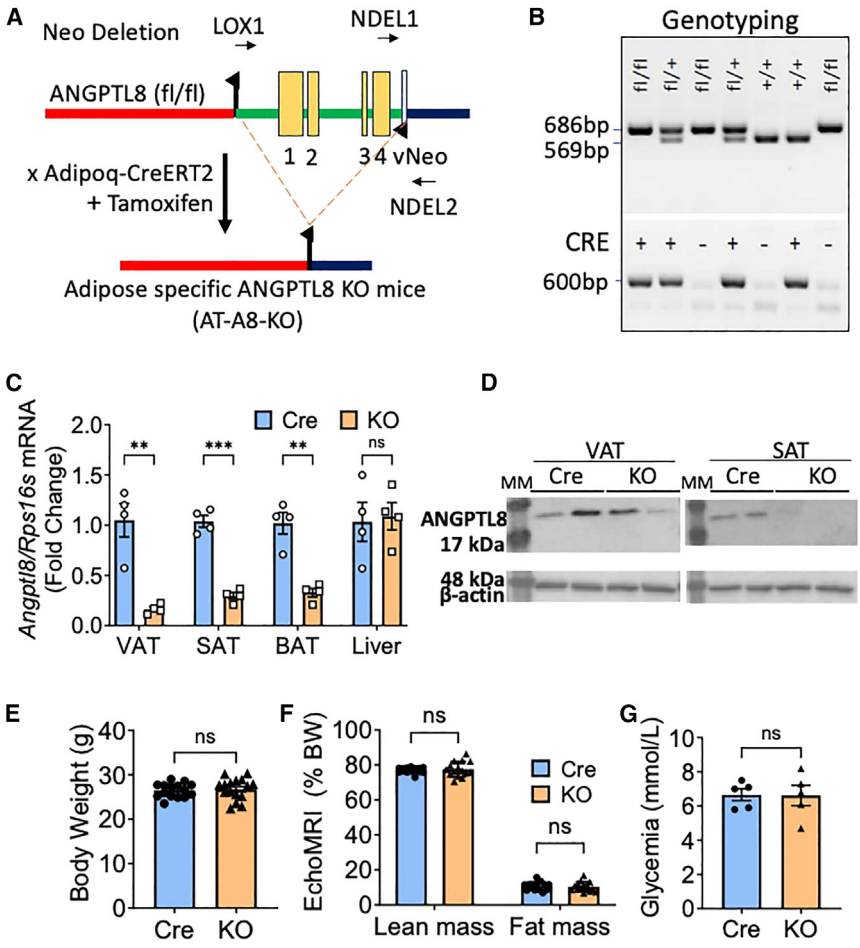

Figure 1. Construction and validation of adipose-specific conditional Angptl8 KO mice

(A) Diagram of the Angptl8 gene with targeted ΔNeo allele, and the disrupted A8 allele. *LoxP* sites were placed upstream of exon 1 and downstream of exon 4. A vNEO cassette was inserted after exon 4. Mice with the targeted ΔNeo allele (Fl/Fl) were crossed with mice expressing Cre under the control of the adiponectin promoter to inactivate A8 in adipocytes (As-A8−/− mice). NDEL1 and NDEL2 primers used for genotyping are indicated.

(B) The presence of the WT, Adipo-Cre transgene or the floxed A8 alleles was evaluated in DNA obtained from ear tissue biopsies using the primers as described in Methods. Specific amplification of a 686 bp DNA fragment corresponds to the floxed-A8 allele while a 569 bp DNA fragment corresponds to the WT A8 allele, the presence of a 600 bp DNA fragment denotes the Adipo-Cre transgene, as verified by genomic PCR.

(C) Angptl8 mRNA expression in VAT, SAT, BAT and Liver tissue ($n = 4$) were measured in 11-week-old male Cre and AT-A8-KO mice, 3 weeks after TMX treatment. Values are means ± SEM. Multiple unpaired t-test for multiple comparison were performed with Holm-Šídák correction using Graphpad Prism 10.

(D) Angptl8 protein expression in collagenase treated mature adipocytes from VAT and SAT tissue in chow diet fed Cre and KO mice (n = 3–4); MM, Pre-stained Molecular weight markers. Quantification are shown in Figure S2B.

(E) Body weight ($n = 15$), (F) lean mass and fat mass, ($n = 15$) and (G) fasted glycemia ($n = 5$) in chow diet fed 11-week-old Cre and AT-A8-KO mice. Data are means ± SEM. Groups were compared using unpaired t-test. For Cre vs. KO: $^{*}p \leq 0.033$, $^{**}p \leq 0.002$, $^{***}p < 0.001$. VAT, visceral adipose tissue; SAT, subcutaneous adipose tissue, BAT, brown adipose tissue.

glycemia of the AT-A8-KO mice, which was lower than that in the Cre mice fed HFHF diet (Figure 2F).

Conditional (embryonic; not inducible) AT-A8 KO mice fed a normal diet were earlier reported to have higher rectal temperature compared to control mice only in fed condition.[7] We found significantly elevated rectal temperature in the inducible AT-A8-KO mice fed HFHF diet compared to Cre mice and also compared to normal diet fed AT-A8-KO mice. However, no such differences were observed between the normal diet fed AT-A8-KO and Cre mice (Figure 2G). Deletion of A8 either in the whole body or specifically in the liver was earlier found to be associated with reduced plasma TG, while the constitutive and conditional (embryonic; not inducible) adipose-specific A8-KO mice under normal diet condition were reported to have significantly higher plasma TG when compared to wildtype or flox/flox mice, which importantly are not appropriate controls.[7,28] However, in the present study with the inducible AT-A8-KO mice, fed normal diet, no significant changes were observed in plasma TG (Figure 2H), liver TG (Figure 2I), plasma cholesterol (Figure 2J), LDL-C/HDL-C ratio (Figure 2K) and free fatty acids (Figure S3A) compared to the control Cre mice. On the other hand, HFHF diet led to decreased liver TG in AT-A8-KO mice compared to Cre mice (Figure 2I) while no changes were noticed in plasma TG (Figure 2H), cholesterol (Figure 2J), LDL/HDL-C ratio (Figure 2K) and free fatty acids (Figure S3A). Only liver TG and plasma cholesterol were elevated in HFHF diet fed Cre-controls and AT-A8-KO mice compared to corresponding normal diet fed mice (Figures 2I and 2J). Measurements in the Comprehensive Lab Animal Monitoring System (CLAMS),[41] showed no apparent overall differences in VO2, VCO2, respiratory exchange ratio (RER) or locomotor activity between Cre and AT-A8-KO mice during a 48-h period as reported earlier,[7] regardless of being on normal or HFHF diet (Figures 3A–3D). However, energy expenditure expressed as a function of metabolic mass[42,43] was significantly higher in the AT-A8-KO mice fed HFHF diet, during the first 5 h of dark phase (12–17 h) on both Day 1 and Day 2 (Figures 3E and 3F), when maximal feeding occurs.[44] The AT-A8-KO mice fed normal diet showed only marginally elevated energy expenditure in the dark phase compared to the Cre controls and the overall energy expenditure in AT-A8-KO mice fed either normal or HFHF diet during the light phase was not statistically different from Cre mice (Figures 3E and 3F).

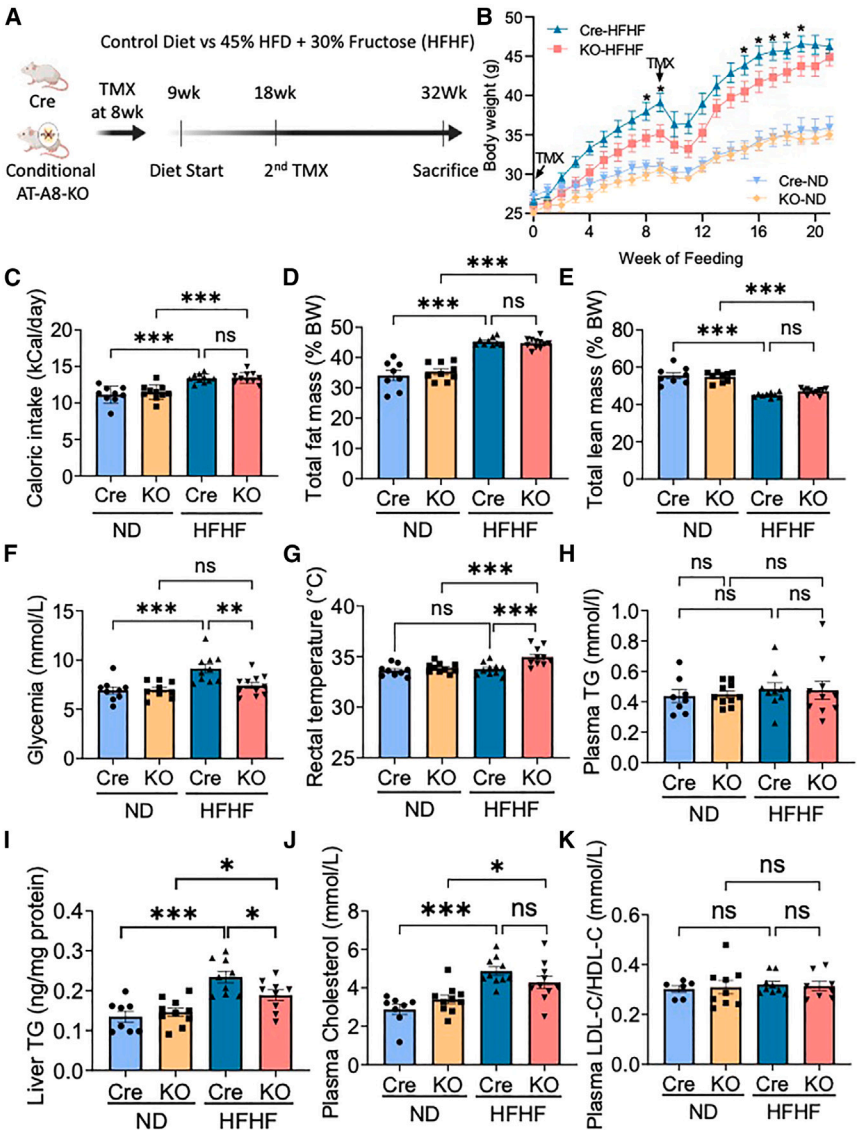

Figure 2. Physiological parameters of AT-A8-KO mice on HFHF diet

(A) Experimental design depicting the timing of TMX treatment and *ad libitum* access to a control diet or high-fat and high-fructose diet (HFHF) for 23-week in Cre and AT-A8-KO mice.

(B) Weekly measurement of body weight in mice from Cre-ND (n = 9), KO-ND (n = 10), Cre-HFHF (n = 10), and KO-HFHF (n = 10) groups. Multiple unpaired t-tests for multiple comparisons were conducted using the Holm-Šídák correction with GraphPad Prism 10. Cre-HFHF vs. KO-HFHF: $^{*}p \leq 0.033$.

(C) Calculation of caloric intake from total food and water intake, measured weekly in Cre and KO mice fed ND or HFHF diet.

(D) Measurement of total fat mass and (E) lean mass using magnetic resonance imaging (EchoMRI) in mice from all four groups after 20 weeks on either the ND or HFHF diet.

(F) Fasted glycemia was measured in 6 h fasted mice. The following were measured in fed condition: (G) rectal temperature, (H) plasma triglycerides (TG), (I) liver TG, (J) plasma cholesterol and (K) ratio of plasma LDL cholesterol and HDL cholesterol, at the study's end in Cre and KO mice fed ND or HFHF diet. Data are means ± SEM. Group comparisons were performed using two-way ANOVA test using GraphPad Prism 10. $^{*}p < 0.05$, $^{**}p < 0.01$, $^{***}p < 0.001$.

AT-A8-KO mice fed HFHF diet show improved glucose tolerance and insulin sensitivity

Constitutive global deletion of A8 in mice was reported to have no impact on glucose tolerance and insulin sensitivity.[28] However, the specific impact of deleting Angptl8 in mature adipocytes on overall glucose homeostasis remained unclear. AT-A8-KO mice on HFHF diet showed markedly improved glucose tolerance and lower insulinemia during an oral glucose tolerance test (OGTT) compared to Cre mice on the same diet (Figures 4A and 4B). The low insulinemia response in the AT-A8-KO mice fed HFHF diet during OGTT was suggestive of better insulin sensitivity. The IPITT showed slightly improved insulin sensitivity in the HFHF diet fed AT-A8-KO mice vs. Cre mice (p = 0.09) (Figure 4C). Glucose tolerance and insulin sensitivity remained unchanged in the AT-A8-KO mice fed normal diet (Figures 4A–4C). Following HFHF diet feeding, HOMA-IR, a marker for insulin resistance, increased in both AT-A8-KO and Cre mice, and there was a trend for this index to be improved in the KO group versus control mice, though it was not statistically significant (Figure 4D).

We further examined if the improved insulin sensitivity seen in the HFHF diet fed AT-A8-KO mice is reflected *ex vivo*, by measuring insulin-stimulated glucose uptake assay using radioactive [^{3}H]-2-DG in the mature adipocytes from VAT and SAT as well as minced whole tissue for BAT and soleus muscle. There were no significant differences in basal or insulin-stimulated glucose uptake between Cre and KO mice on the HFHF diet in the adipocytes from VAT, whereas there was a significant increase in the glucose uptake in the SAT adipocytes and BAT from AT-A8-KO mice (Figures 4E and 4F). There was no difference between the Cre controls and AT-A8-KO mice in the expression levels of Glut4 mRNA, the major glucose transporter in all the three adipose depots (Figure S4A). There was no change in the basal or insulin stimulated glucose uptake in the soleus from AT-A8-KO mice (Figure S2C). Overall, these results indicate that specific deletion of A8 in adipose tissue in adult mice reduces HFHF diet induced glucose intolerance and insulin resistance.

Adipose tissue characteristics in AT-A8-KO mice

After 23 weeks on either a normal diet or HFHF diet, fat depots were dissected from the mice and examined for morphological changes. Although the HFHF diet led to an increase in adipose tissue mass across all the three fat depots, there were no

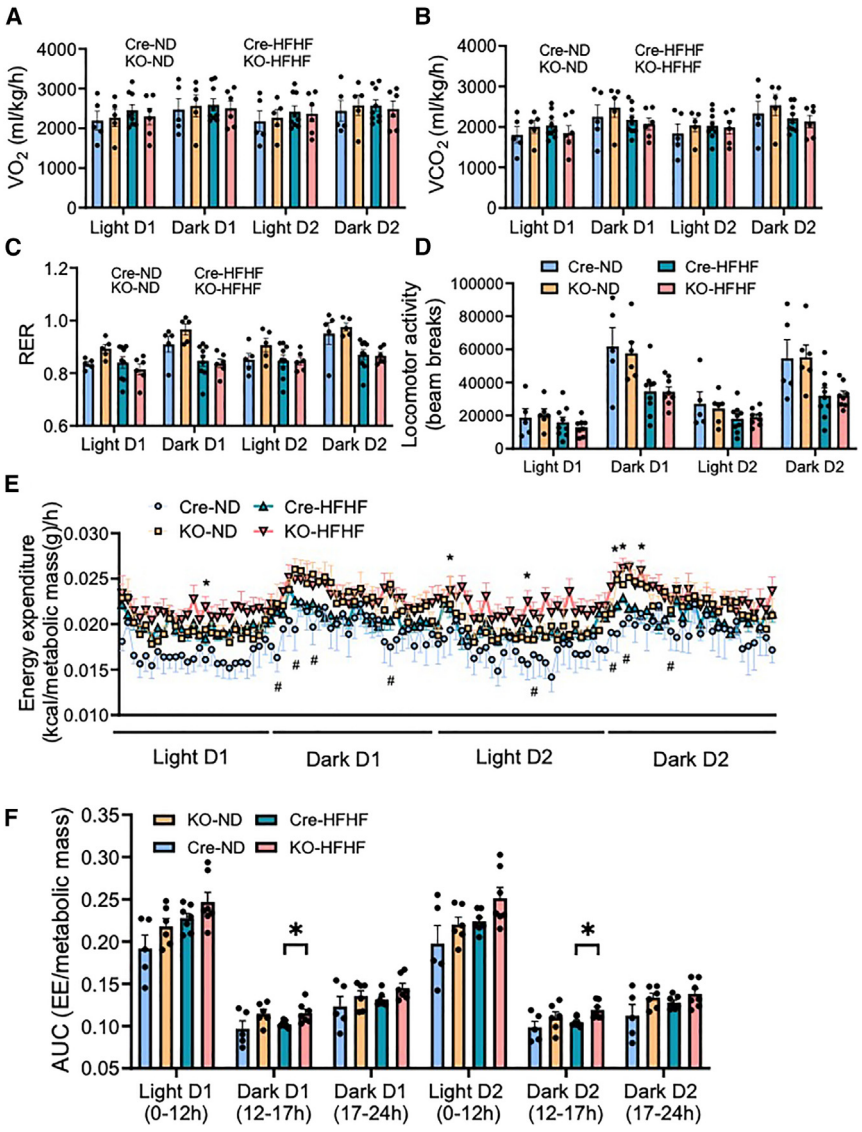

Figure 3. Increased energy expenditure in early dark cycle in HFHF diet fed AT-A8-KO mice

(A) Male mice from Cre-ND (n = 5), KO-ND (n = 5), Cre-HFHF (n = 7–9), and KO-HFHF (n = 7–8) were housed individually in metabolic cages for three days at room temperature (22°C). After 24h of adaptation, both O2 consumption and (B) CO2 output (C) RER and (D) Locomotor activity were measured for 2 consecutive days and divided into Light D1, Dark D1, Light D2 and Dark D2 cycle. Values are means ± SEM. Two-way ANOVA with Tukey's multiple comparisons test were performed using GraphPad Prism 10. *$p \leq 0.05$.

(E) Energy expenditure was calculated and expressed as kcal/metabolic mass(g)/h.

(F) Area under the curve were calculated from energy expenditure graphs and divided as follows: Light D1 (0-12h), Dark D1 (12-17h), Dark D1 (17-24h), Light D2 (0-12h), Dark D1 (12-17h) and Dark D2 (17-24h). Two-way ANOVA with Tukey's multiple comparisons test were performed using GraphPad Prism 10. *$p < 0.033$.

discernible differences between Cre and AT-A8-KO mice (Figure 5A). Histological examination revealed an increase in VAT and SAT cell size in both Cre and AT-A8-KO mice on the HFHF diet compared to the normal diet (Figure 5B). There were no differences among the groups in the cell size or morphology of the BAT depots (Figure 5B). In the normal diet fed mice, the AT-A8-KO mice displayed a slightly higher proportion of the smaller adipocytes in the SAT and VAT compared to Cre mice; however, this difference was lost in HFHF diet fed mice (Figures 5B, 5C, S3B and S3C). BAT cell size distribution did not change among groups on either diet (Figure 5C). We further observed that there were no changes in the expression of browning markers, UCP1, PRDM16, PPPARGC1A and the corresponding transcription factors PPARα and PPARγ in the VAT and SAT from HFHF diet fed AT-A8-KO mice, compared to control Cre mice (Figures S4B and S4C). These brown adipocyte markers also did not change in the BAT from the AT-A8-KO mice (Figures S4B and S4C). Lack of any major effect on the expression of browning markers in the white adipose tissue was also reported earlier in adipose specific-A8-KO mice.[7]

HFHF diet fed AT-A8-KO mice show reduced levels of inflammatory markers

In order to better understand the underlying causes for the partial protection from diet-induced insulin resistance in the AT-A8-KO mice, we examined adipose macrophage infiltration as they are known to modulate insulin sensitivity. During high fat diet induced adipose expansion, macrophages are drawn to the adipose tissue to promote adipose inflammation and associated disturbances in insulin action.[45–48] Adipose tissue macrophages (ATMs) actively participate in recruiting additional macrophages by releasing chemokines such as MCP-1 and MIP-1α, leading to the formation of Crown-Like Structures (CLS) around deceased adipocytes.[49,50] We examined for the presence of CLS using CLS positive marker MAC-2[51,52] in the VAT and the results showed significantly fewer CLS in the HFHF diet fed AT-A8-KO mice compared to Cre mice (Figures 6A and 6B). Furthermore, plasma MCP-1 levels surged in the Cre mice following HFHF diet compared to the normal diet but not in the AT-A8-KO mice, and also there was a significant decline in the plasma MCP-1 in the AT-A8-KO mice compared to Cre controls, fed HFHF diet (Figure 6C). Plasma leptin levels increased in both the Cre and AT-A8-KO mice following HFHF diet, though the increase in the AT-A8-KO mice was modest and significantly lower than in the Cre control group (Figure 6D). There were no marked genotype or diet related changes in plasma IL-6, TNF-α (Figures S3D and S3E) and adiponectin

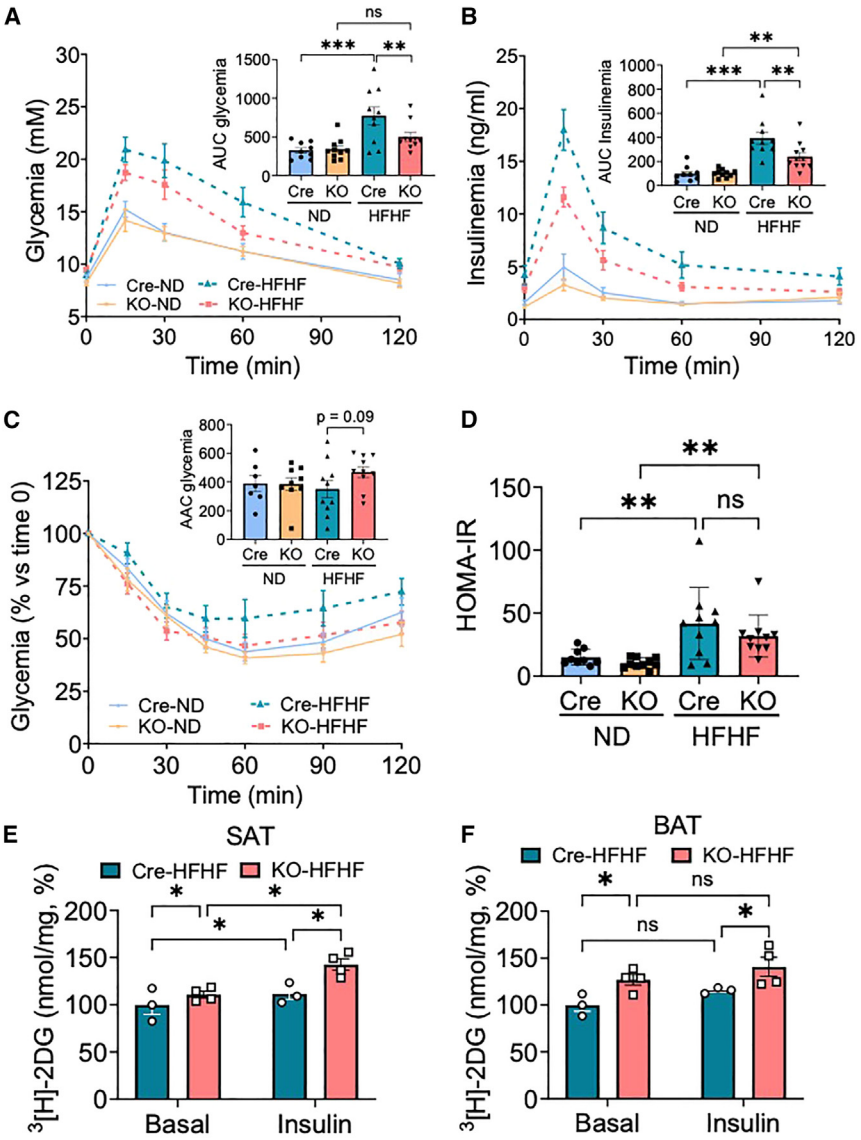

Figure 4. Improved Glucose Tolerance and Insulin Sensitivity in AT-A8-KO Mice on HFHF Diet

(A) Male mice from Cre-ND (n = 9), KO-ND (n = 10), Cre-HFHF (n = 10), and KO-HFHF (n = 10) groups, 20 weeks after ND or HFHF diet feeding, were subject to oral glucose tolerance test (OGTT) after a 6h fasting. Area under curve (AUC) during the OGTT was calculated.

(B) Tail blood was collected at indicated times during the OGTT and analyzed for insulin by AlphaLISA and AUC for insulinemia was calculated.

(C) Insulin tolerance test (ITT) was conducted after 23 weeks of ND or HFHF diet feeding in all four groups as indicated, following 6 h fasting. Area above curve (AAC) and (D) HOMA-IR were calculated in these mice. Values are means ± SEM. Groups were compared by two-way ANOVA test using GraphPad Prism 10. *p < 0.033, **p < 0.01, ***p < 0.001.

(E) *ex vivo* basal or insulin stimulated glucose uptake measurements were done using radioactive [^{3}H]-2-deoxy-D-glucose in SAT mature adipocytes and (F) BAT tissues isolated from Cre (n = 3) and KO (n = 4) mice on HFHF diet. Data are means ± SEM. Two-way ANOVA with Tukey's multiple comparisons test was applied using GraphPad Prism 10. *$p \leq 0.033$.

(Figure 6E), among the different groups of mice. In addition, we noticed that the expression of adiponectin (Adipoq) is unchanged in the three adipose depots from the HFHF diet fed AT-A8-KO mice, compared to Cre controls (Figure S4D). Similar results were obtained for the expression of IL6 and TNFα, except for the decreased expression of TNFα in SAT from AT-A8-KO mice (Figure S4E). These findings collectively suggest an overall reduction in macrophage infiltration and possibly the associated inflammation in the VAT of AT-A8-KO mice fed HFHF diet.

Effect of AT-A8-KO on ANGPTL4 and ANGPTL8 expression in adipose depots and plasma A8 levels in the HFHF diet fed mice

We further examined if deletion of A8 in adipose tissue alters the expression of ANGPTL4, which is known to bind and inhibit LPL and also with A8, which releases A4 inhibition of LPL. Results showed no effect on the mRNA expression of ANGPTL4 in the three adipose depots while there was a significant reduction in A8 mRNA levels, as expected (Figure S5A). Unaltered plasma A8 levels in the AT-A8-KO mice fed HFHF diet, compared to Cre controls (Figure S5B), suggested that adipose A8 does not significantly contribute to plasma A8 levels and has no direct effect on plasma LPL activity.

DISCUSSION

Here we demonstrate that adipose A8 contributes to the regulation of whole body glucose and energy metabolism, as well as adipose inflammation under an obesogenic nutritional stress condition.

We employed mice with tamoxifen-inducible deletion of adipose A8 to avoid any possible developmental effects arising from deletion constitutively or conditionally at embryonic stage, which could have altered the whole-body response in terms of fat accretion and body weight gain. Indeed, it has been shown before that adiponectin promoter is active by embryonic day 11–16[53–55] and that A8 likely plays an important role in fetal development.[56] Thus, it is necessary to dissect-out and avoid any possible developmental effects while studying the significance of A8 in mature adipocytes. Thus we did not notice any effects on either body weight, fat or lean mass and fasting glycemia in the normal diet fed AT-A8-KO male mice compared to control Cre mice, unlike what was shown before in 18–22 weeks old female mice and 8–10 weeks old male mice with constitutive global deletion of adipose Angptl8.[28,29] Lack of adipose A8 in the

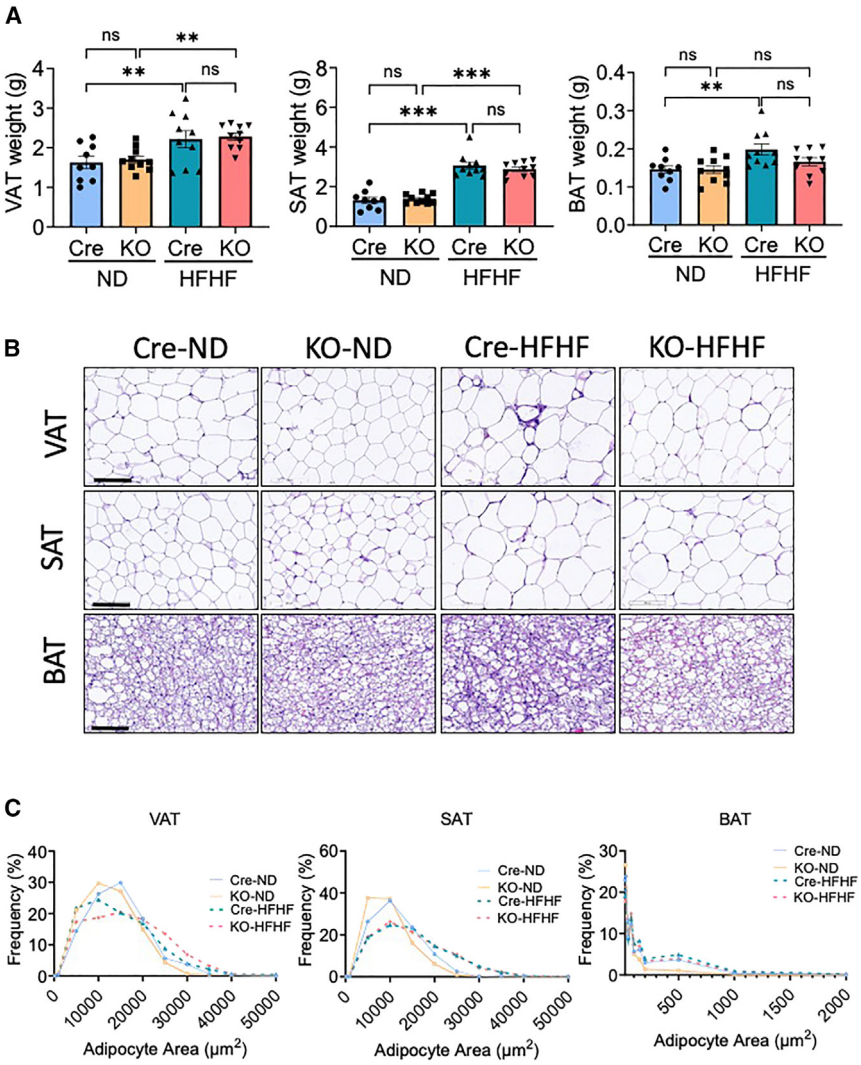

Figure 5. Adipose tissue mass, morphology and cell size

(A) Tissue weights of fat pads (VAT, SAT, BAT) from Cre and KO mice on ND and HFHF diet for 23 weeks (n = 9–10/genotype). Values are means ± SEM. Groups were compared using two-way ANOVA test using GraphPad Prism 10. *$p < 0.05$, ***$p < 0.001$.

(B) Representative H&E staining of tissue sections (n = 4–6/genotype, original magnification ×20; scale bar = 200 μm).

(C) Adipocyte size was quantified using ImageJ software (4 fields/tissue section) and presented as the frequency distribution of adipocyte cell/lipid droplet size, expressed as percentage.

adult mice is slightly protective against HFHF diet induced weight gain, for several weeks on HFHF diet. However, this protection waned out by chronic HFHF diet feeding (23 weeks), even though there was no re-emergence of A8 expression due to increased generation of adipocytes as we administered a second round of TMX after 8–9 weeks of feeding. As noticed with the normal diet fed AT-A8-KO mice, in the chronic HFHF diet fed AT-A8-KO mice also there were no changes in lean and fat mass, fat pad weights and liver weight, and TG and plasma lipids. This suggests that over an extended period of obesogenic diet, there can be compensatory effects, perhaps originating from liver A8 in the AT-A8-KO mice, obliterating protective effects of adipose A8 deletion on the body weight gain cause by the HFHF diet.

Depending on the experimental conditions and the genetic background of the mice, either whole-body or liver or adipose specific deletion of A8 was reported to have varying effects on glucose homeostasis and insulin sensitivity.[28,39,57–59] However, the precise role of adipose A8 on glucose and insulin homeostasis under *in vivo* conditions was not clear from these earlier studies. Here we provide evidence that adipose A8 plays a role in the control of insulin sensitivity. The lower fasting glycemia in the HFHF diet fed AT-A8-KO mice compared to the control Cre mice, suggestive of better glucose and insulin homeostasis, is confirmed by the improved glucose tolerance and lower insulin secretion in response to the glucose load. Moreover, the insulin stimulated glucose uptake was found to be higher in the subcutaneous and brown adipose depots from the AT-A8-KO mice, despite the unaltered expression of Glut4, the major insulin-regulated glucose transporter in the adipose tissues,[60] which further supports a role for A8 in insulin signaling and glucose homeostasis.

It was reported that normal diet fed mice with a deletion of A8 either in the whole body or in adipose tissue, but not in the liver, show elevated rectal temperature under fed conditions.[7] This suggested that A8, specifically in adipose depots regulates a thermogenic program, depending on the nutritional state. Unlike the earlier studies where comparisons were made between adipose-A8-KO mice and Fl/Fl mice, which are not appropriate controls,[7] the elevated rectal temperature was seen here only in the HFHF diet fed AT-A8-KO mice, while normal diet fed AT-A8-KO mice did not show any changes, compared to the Cre controls. It is important to note that the appropriate controls for the adipose tissue specific A8-KO mice are not wildtype or Fl/Fl mice, but the corresponding Cre-transgenic mice. Moreover, examination of energy expenditure in these mice in CLAMS revealed that during early dark phase, when maximal feeding occurs,[45] the AT-A8-KO mice showed higher levels of energy expenditure compared to Cre controls, and this difference was more marked in the HFHF diet fed mice. Thus, feeding is known to be associated with elevated energy expenditure[29,61] and the increased energy expenditure in the HFHF diet fed AT-A8-KO mice may explain the increased body temperature that may be due to elevated oxidative metabolism in the subcutaneous and brown adipose tissue depots. However,

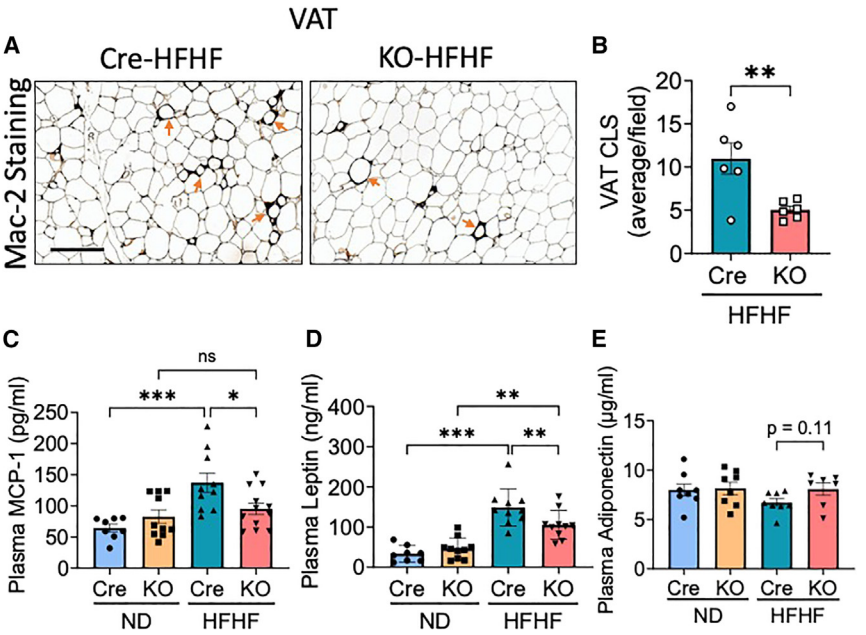

Figure 6. AT-A8-KO Mice on HFHF diet Reduces Inflammatory Markers

(A) MAC-2 immunostaining in VAT tissue section from Cre and KO mice on HFHF diet and (B) quantification of crown-like structures (CLS) ($n = 6$ mice, 4 fields/tissue section, original magnification × 20; scale bar = 400 µm). Values are means ± SEM and groups were compared using unpaired t-test. $^{**}p \leq 0.002$. (C) Plasma MCP-1, (D) Leptin and (E) Adiponectin levels in mice under fed state were quantified by ELISA or AlphaLISA (n = 8–10). Values are means ± SEM. Groups were compared using two-way ANOVA test using GraphPad Prism 10. $^{*}p \leq 0.033$, $^{**}p \leq 0.002$, $^{***}p < 0.001$.

as there was no enhanced expression of browning markers in the SAT or VAT in the AT-A8-KO mice, the precise mechanism whereby adipose A8 regulates energy expenditure and glucose homeostasis under nutri-stress remains to be established.

ANGPTL8 has also been implicated in proinflammatory processes.[62–64] We noticed that AT-A8-KO mice on the obesogenic HFHF diet exhibited signs of reduced inflammation, including decreased crown-like structures (CLS) in VAT and lower levels of plasma MCP-1, a proinflammatory factor, compared to the control Cre mice, suggesting reduced macrophage infiltration in the adipose tissue. Moreover, AT-A8-KO mice on the HFHF diet exhibited a marked decrease in plasma leptin levels, while plasma adiponectin levels were only marginally elevated. Considering that leptin has proinflammatory role[65] whereas adiponectin is an anti-inflammatory factor,[66] the inverse changes in these adipokines in the HFHF diet fed AT-A8-KO mice can partly explain the reduced inflammation in these mice compared to control Cre mice. Furthermore, MCP-1, which is expressed in adipocytes and induced by obese conditions and high fat diet, is a known trigger for macrophage infiltration in the adipose tissue,[67,68] and its expression is regulated by the pro-inflammatory transcription factor NF-κB.[69] Indeed, A8 has been shown to activate the NF-κB signaling and promote extracellular matrix degradation and inflammatory cytokine release, whereas A8 inhibition reduced NF-κB signaling.[63] Thus, deletion of A8 in the adipose tissue may protect from diet induced inflammation by preventing NF-κB activation, reducing MCP-1 production, macrophage infiltration and CLS formation. The reduced adipose inflammation and decreased macrophage infiltration might contribute to overall healthy adipocytes[70–72] and promote better insulin sensitivity.[45–48]

Limitations of the study

Even though this study offers valuable insight into the role of adipose A8 in regulating metabolism and inflammation under long term nutri-stress, there are a few limitations to consider. This study included only male mice and thus any possible different effects of adipose-A8 deletion on female mice are not addressed. Females are known to be less prone to the effects of diet-induced obesity, and yet it may be interesting to assess what effects A8 has in female mice. We also did not examine the phenotype of adipose-A8-KO mice under fasting and refeeding conditions. Since A8 is highly induced by feeding and reduced by fasting, examining these effects on adipose A8 could provide additional insights. The fasting/refeeding induced changes in plasma Angptl8 levels, which control plasma LPL activity, are more reflected by A8 secreted from liver rather than from adipose tissue.[8,9,27,35,73] Therefore, we did not focus on the effects of fasting/refeeding on adipose A8 functions but only under fed conditions, which is also a physiological situation. Nevertheless, it would be of interest in future work to study the phenotype of adipose A8 KO mice also under fasting/refeeding as A8 is also induced by this condition. Future studies are needed to investigate the mechanisms by which adipose A8 regulates systemic glucose and energy metabolism or reduces inflammation under obesogenic diet, which is not the focus of the present study. The possible mechanisms by which A8 deletion in adipose tissue causes the noted phenotypes is uncertain. It is possible that some, if not all, the observed phenotypes could be a result of changes in LPL activity in adipose tissue. This as well as other potential mechanisms remain to be investigated.

Conclusions

In conclusion, the results indicate that adipose A8 has a role to play in whole body energy and glucose homeostasis in the context of nutritional stress as deletion of adipose A8 in adult male mice fed an obesogenic HFHF diet reduces obesity, enhances postprandial adipose thermogenesis, improves glucose tolerance and reduces inflammation, thereby promoting an overall healthy obese phenotype. Several earlier reports indicated the possible therapeutic implications of curtailing circulating A8 in conditions of obesity and associated triglyceridemia. Our present results suggest that inhibiting adipose Angptl8 alone can also have beneficial effects, particularly under obesogenic conditions. Thus, any potential therapeutics to blockade A8 function

in the whole body could be designed not only to inhibit the circulating A8, but also in adipose tissue, *in situ*. Such A8 inhibitors may be effective for the treatment of obesity and hypertriglyceridemia, and also to imrove insulin sensitivity and inflammation.

RESOURCE AVAILABILITY

Lead contact

Further information and requests for resources and reagents should be directed to and will be fulfilled by the corresponding author Marc Prentki (marc.prentki@umontreal.ca).

Materials availability statement

This study did not generate new unique reagents. Further information and requests for resources such as reagents listed in key resources table should be directed to the corresponding author Marc Prentki (marc.prentki@umontreal.ca).

Data and code availability

- Data: No additional data other than that reported in the manuscript is associated with this study. Further information and requests for any data reported in the manuscript should be directed to the corresponding author Marc Prentki (marc.prentki@umontreal.ca).
- Code: This study did not generate any original code.

ACKNOWLEDGMENTS

This work was supported by funds from the Dasman Diabetes Research Institute/Montreal Medical International (to M.P., S.R.M.M., R.S., M.A-F., J.A., F.A-M.). We thank the core facilities and the animal house facility of CRCHUM. The graphics were created with BioRender.com.

AUTHOR CONTRIBUTIONS

AG, MAF, SRMM, and MP designed research; AG, IC, YHL, AKO, and IAK performed research; AG, IC, MAF, JA, FAM, MLP, SRMM and MP analyzed data; and AG, SRMM, and MP wrote the paper.

DECLARATION OF INTERESTS

The authors declare that they have no known competing financial interests or personal relationships that could have appeared to influence the work reported in this paper.

STAR★METHODS

Detailed methods are provided in the online version of this paper and include the following:

- KEY RESOURCES TABLE
- EXPERIMENTAL MODEL
- METHOD DETAILS
  - Generation of adipose-specific ANGPTL8 conditional KO mice and breeding strategy
  - High-fat high-fructose diet-induced obesity
  - Metabolic studies using Comprehensive Lab Animal Monitoring System (CLAMS)
  - Oral glucose tolerance test
  - Insulin tolerance test
  - Glucose uptake assay
  - Plasma parameters
  - Tissue histology and analysis
  - Immunoblotting
  - RNA extraction and quantitative PCR
- QUANTIFICATION AND STATISTICAL ANALYSIS

SUPPLEMENTAL INFORMATION

Supplemental information can be found online at https://doi.org/10.1016/j.isci.2024.111292.

Received: April 8, 2024
Revised: August 28, 2024
Accepted: October 28, 2024
Published: November 9, 2024

REFERENCES

1. Rosen, E.D., and Spiegelman, B.M. (2014). What we talk about when we talk about fat. Cell *156*, 20–44. https://doi.org/10.1016/j.cell.2013.12.012.
2. Wong, R.H.F., and Sul, H.S. (2010). Insulin signaling in fatty acid and fat synthesis: a transcriptional perspective. Curr. Opin. Pharmacol. *10*, 684–691. https://doi.org/10.1016/j.coph.2010.08.004.
3. Wang, H., and Eckel, R.H. (2009). Lipoprotein lipase: from gene to obesity. Am. J. Physiol. Endocrinol. Metab. *297*, E271–E288. https://doi.org/10.1152/ajpendo.90920.2008.
4. Kuwajima, M., Foster, D.W., and McGarry, J.D. (1988). Regulation of lipoprotein lipase in different rat tissues. Metabolism *37*, 597–601. https://doi.org/10.1016/0026-0495(88)90178-3.
5. Lithell, H., Boberg, J., Hellsing, K., Lundqvist, G., and Vessby, B. (1978). Lipoprotein-lipase activity in human skeletal muscle and adipose tissue in the fasting and the fed states. Atherosclerosis *30*, 89–94. https://doi.org/10.1016/0021-9150(78)90155-7.
6. Wang, Y., McNutt, M.C., Banfi, S., Levin, M.G., Holland, W.L., Gusarova, V., Gromada, J., Cohen, J.C., and Hobbs, H.H. (2015). Hepatic ANGPTL3 regulates adipose tissue energy homeostasis. Commun.Biol. *112*, 11630–11635. https://doi.org/10.1073/pnas.1515374112.
7. Oldoni, F., Cheng, H., Banfi, S., Gusarova, V., Cohen, J.C., and Hobbs, H.H. (2020). ANGPTL8 has both endocrine and autocrine effects on substrate utilization. JCI Insight *5*, e138777. https://doi.org/10.1172/jci.insight.138777.
8. Zhang, R., and Zhang, K. (2022). An updated ANGPTL3-4-8 model as a mechanism of triglyceride partitioning between fat and oxidative tissues. Prog. Lipid Res. *85*, 101140. https://doi.org/10.1016/j.plipres.2021.101140.
9. Kersten, S. (2019). New insights into angiopoietin-like proteins in lipid metabolism and cardiovascular disease risk. Curr. Opin. Lipidol. *30*, 205–211. https://doi.org/10.1097/MOL.0000000000000600.
10. Quagliarini, F., Wang, Y., Kozlitina, J., Grishin, N.V., Hyde, R., Boerwinkle, E., Valenzuela, D.M., Murphy, A.J., Cohen, J.C., and Hobbs, H.H. (2012). Atypical angiopoietin-like protein that regulates ANGPTL3. Proc Natl Acad Sci USA *109*, 19751–19756. https://doi.org/10.1073/pnas.1217552109.
11. Koster, A., Chao, Y.B., Mosior, M., Ford, A., Gonzalez-DeWhitt, P.A., Hale, J.E., Li, D., Qiu, Y., Fraser, C.C., Yang, D.D., et al. (2005). Transgenic angiopoietin-like (angptl)4 overexpression and targeted disruption of angptl4 and angptl3: regulation of triglyceride metabolism. Endocrinology *146*, 4943–4950. https://doi.org/10.1210/en.2005-0476.
12. Shimizugawa, T., Ono, M., Shimamura, M., Yoshida, K., Ando, Y., Koishi, R., Ueda, K., Inaba, T., Minekura, H., Kohama, T., and Furukawa, H. (2002). ANGPTL3 decreases very low density lipoprotein triglyceride clearance by inhibition of lipoprotein lipase. J. Biol. Chem. *277*, 33742–33748. https://doi.org/10.1074/jbc.M203215200.
13. Yoshida, K., Shimizugawa, T., Ono, M., and Furukawa, H. (2002). Angiopoietin-like protein 4 is a potent hyperlipidemia-inducing factor in mice and inhibitor of lipoprotein lipase. J. Lipid Res. *43*, 1770–1772. https://doi.org/10.1194/jlr.c200010-jlr200.
14. Romeo, S., Yin, W., Kozlitina, J., Pennacchio, L.A., Boerwinkle, E., Hobbs, H.H., and Cohen, J.C. (2009). Rare loss-of-function mutations in ANGPTL family members contribute to plasma triglyceride levels in humans. J. Clin. Invest. *119*, 70–79. https://doi.org/10.1172/JCI37118.

15. Abu-Farha, M., Alatrach, M., Abubaker, J., Al-Khairi, I., Cherian, P., Agyin, K., Abdelgani, S., Norton, L., Adams, J., Al-Saeed, D., et al. (2023). Plasma insulin is required for the increase in plasma angiopoietin-like protein 8 in response to nutrient ingestion. Diabetes. Metab. Res. Rev. *39*, e3643. https://doi.org/10.1002/dmrr.3643.

16. Zhang, R. (2012). Lipasin, a novel nutritionally-regulated liver-enriched factor that regulates serum triglyceride levels. Biochem. Biophys. Res. Commun. *424*, 786–792. https://doi.org/10.1016/j.bbrc.2012.07.038.

17. Ren, G., Kim, J.Y., and Smas, C.M. (2012). Identification of RIFL, a novel adipocyte-enriched insulin target gene with a role in lipid metabolism. Am. J. Physiol. Endocrinol. Metab. *303*, E334–E351. https://doi.org/10.1152/ajpendo.00084.2012.

18. Chen, Y.Q., Pottanat, T.G., Siegel, R.W., Ehsani, M., Qian, Y.W., Zhen, E.Y., Regmi, A., Roell, W.C., Guo, H., Luo, M.J., et al. (2020). Angiopoietin-like protein 8 differentially regulates ANGPTL3 and ANGPTL4 during postprandial partitioning of fatty acids. J. Lipid Res. *61*, 1203–1220. https://doi.org/10.1194/jlr.RA120000781.

19. Chi, X., Britt, E.C., Shows, H.W., Hjelmaas, A.J., Shetty, S.K., Cushing, E.M., Li, W., Dou, A., Zhang, R., and Davies, B.S.J. (2017). ANGPTL8 promotes the ability of ANGPTL3 to bind and inhibit lipoprotein lipase. Mol. Metabol. *6*, 1137–1149. https://doi.org/10.1016/j.molmet.2017.06.014.

20. Haller, J.F., Mintah, I.J., Shihanian, L.M., Stevis, P., Buckler, D., Alexa-Braun, C.A., Kleiner, S., Banfi, S., Cohen, J.C., Hobbs, H.H., et al. (2017). ANGPTL8 requires ANGPTL3 to inhibit lipoprotein lipase and plasma triglyceride clearance. J. Lipid Res. *58*, 1166–1173. https://doi.org/10.1194/jlr.M075689.

21. Kovrov, O., Kristensen, K.K., Larsson, E., Ploug, M., and Olivecrona, G. (2019). On the mechanism of angiopoietin-like protein 8 for control of lipoprotein lipase activity. J. Lipid Res. *60*, 783–793. https://doi.org/10.1194/jlr.M088807.

22. Chen, Y.Q., Zhen, E.Y., Russell, A.M., Ehsani, M., Siegel, R.W., Qian, Y., and Konrad, R.J. (2023). Decoding the role of angiopoietin-like protein 4/8 complex-mediated plasmin generation in the regulation of LPL activity. J. Lipid Res. *64*, 100441. https://doi.org/10.1016/j.jlr.2023.100441.

23. Zhen, E.Y., Chen, Y.Q., Russell, A.M., Ehsani, M., Siegel, R.W., Qian, Y., and Konrad, R.J. (2023). Angiopoietin-like protein 4/8 complex-mediated plasmin generation leads to cleavage of the complex and restoration of LPL activity. Proc Natl Acad Sci USA *120*, e2214081120. https://doi.org/10.1073/pnas.2214081120.

24. Ruppert, P.M.M., Michielsen, C.C.J.R., Hazebroek, E.J., Pirayesh, A., Olivecrona, G., Afman, L.A., and Kersten, S. (2020). Fasting induces ANGPTL4 and reduces LPL activity in human adipose tissue. Mol. Metabol. *40*, 101033. https://doi.org/10.1016/j.molmet.2020.101033.

25. Kersten, S. (2021). Role and mechanism of the action of angiopoietin-like protein ANGPTL4 in plasma lipid metabolism. J. Lipid Res. *62*, 100150. https://doi.org/10.1016/j.jlr.2021.100150.

26. Koishi, R., Ando, Y., Ono, M., Shimamura, M., Yasumo, H., Fujiwara, T., Horikoshi, H., and Furukawa, H. (2002). Angptl3 regulates lipid metabolism in mice. Nat. Genet. *30*, 151–157. https://doi.org/10.1038/ng814.

27. Sylvers-Davie, K.L., and Davies, B.S.J. (2021). Regulation of lipoprotein metabolism by ANGPTL3, ANGPTL4, and ANGPTL8. Am. J. Physiol. Endocrinol. Metab. *321*, E493–E508. https://doi.org/10.1152/ajpendo.00195.2021.

28. Wang, Y., Quagliarini, F., Gusarova, V., Gromada, J., Valenzuela, D.M., Cohen, J.C., and Hobbs, H.H. (2013). Mice lacking ANGPTL8 (Betatrophin) manifest disrupted triglyceride metabolism without impaired glucose homeostasis. Proc Natl Acad Sci USA *110*, 16109–16114. https://doi.org/10.1073/pnas.1315292110.

29. Banfi, S., Gusarova, V., Gromada, J., Cohen, J.C., and Hobbs, H.H. (2018). Increased thermogenesis by a noncanonical pathway in ANGPTL3/8-deficient mice. Proceedings of the National Academy of Sciences *115*, E1249–E1258. https://doi.org/10.1073/pnas.1717420115.

30. Ghosh, A., Leung, Y.H., Yu, J., Sladek, R., Chénier, I., Oppong, A.K., Peyot, M.L., Madiraju, S.R.M., Al-Khairi, I., Thanaraj, T.A., et al. (2024). Silencing ANGPTL8 reduces mouse preadipocyte differentiation and insulin signaling. Biochim. Biophys. Acta Mol. Cell Biol. Lipids *1869*, 159461. https://doi.org/10.1016/j.bbalip.2024.159461.

31. Abu-Farha, M., Madhu, D., Hebbar, P., Mohammad, A., Channanath, A., Kavalakatt, S., Alam-Eldin, N., Alterki, F., Taher, I., Alsmadi, O., et al. (2023). The Proinflammatory Role of ANGPTL8 R59W Variant in Modulating Inflammation through NF-kappaB Signaling Pathway under TNFalpha Stimulation. Cells *12*, 2563. https://doi.org/10.3390/cells12212563.

32. Zhang, Y., Guo, X., Yan, W., Chen, Y., Ke, M., Cheng, C., Zhu, X., Xue, W., Zhou, Q., Zheng, L., et al. (2017). ANGPTL8 negatively regulates NF-kappaB activation by facilitating selective autophagic degradation of IKK-gamma. Nat. Commun. *8*, 2164. https://doi.org/10.1038/s41467-017-02355-w.

33. Mysore, R., Liebisch, G., Zhou, Y., Olkkonen, V.M., and Nidhina Haridas, P.A. (2017). Angiopoietin-like 8 (Angptl8) controls adipocyte lipolysis and phospholipid composition. Chem. Phys. Lipids *207*, 246–252. https://doi.org/10.1016/j.chemphyslip.2017.05.002.

34. Chen, S., Feng, M., Zhang, S., Dong, Z., Wang, Y., Zhang, W., and Liu, C. (2019). Angptl8 mediates food-driven resetting of hepatic circadian clock in mice. Nat. Commun. *10*, 3518. https://doi.org/10.1038/s41467-019-11513-1.

35. Abu-Farha, M., Ghosh, A., Al-Khairi, I., Madiraju, S.R.M., Abubaker, J., and Prentki, M. (2020). The multi-faces of Angptl8 in health and disease: Novel functions beyond lipoprotein lipase modulation. Prog. Lipid Res. *80*, 101067. https://doi.org/10.1016/j.plipres.2020.101067.

36. Abu-Farha, M., Abubaker, J., and Tuomilehto, J. (2017). ANGPTL8 (betatrophin) role in diabetes and metabolic diseases. Diabetes. Metab. Res. Rev. *33*, e2919. https://doi.org/10.1002/dmrr.2919.

37. Li, D.P., Huang, L., Kan, R.R., Meng, X.Y., Wang, S.Y., Zou, H.J., Guo, Y.M., Luo, P.Q., Pan, L.M., Xiang, Y.X., et al. (2023). LILRB2/PirB mediates macrophage recruitment in fibrogenesis of nonalcoholic steatohepatitis. Nat. Commun. *14*, 4436. https://doi.org/10.1038/s41467-023-40183-3.

38. Abu-Farha, M., Abubaker, J., Al-Khairi, I., Cherian, P., Noronha, F., Hu, F.B., Behbehani, K., and Elkum, N. (2015). Higher plasma betatrophin/ANGPTL8 level in Type 2 Diabetes subjects does not correlate with blood glucose or insulin resistance. Sci. Rep. *5*, 10949. https://doi.org/10.1038/srep10949.

39. Gusarova, V., Banfi, S., Alexa-Braun, C.A., Shihanian, L.M., Mintah, I.J., Lee, J.S., Xin, Y., Su, Q., Kamat, V., Cohen, J.C., et al. (2017). ANGPTL8 Blockade With a Monoclonal Antibody Promotes Triglyceride Clearance, Energy Expenditure, and Weight Loss in Mice. Endocrinology *158*, 1252–1259. https://doi.org/10.1210/en.2016-1894.

40. Zhang, H., Léveillé, M., Courty, E., Gunes, A., N Nguyen, B., and Estall, J.L. (2020). Differences in metabolic and liver pathobiology induced by two dietary mouse models of nonalcoholic fatty liver disease. Am. J. Physiol. Endocrinol. Metab. *319*, E863–E876. https://doi.org/10.1152/ajpendo.00321.2020.

41. Poursharifi, P., Attané, C., Mugabo, Y., Al-Mass, A., Ghosh, A., Schmitt, C., Zhao, S., Guida, J., Lussier, R., Erb, H., et al. (2020). Adipose ABHD6 regulates tolerance to cold and thermogenic programs. JCI Insight *5*, e140294. https://doi.org/10.1172/jci.insight.140294.

42. Even, P.C., and Nadkarni, N.A. (2012). Indirect calorimetry in laboratory mice and rats: principles, practical considerations, interpretation and perspectives. Am. J. Physiol. Regul. Integr. Comp. Physiol. *303*, R459–R476. https://doi.org/10.1152/ajpregu.00137.2012.

43. Zhao, S., Mugabo, Y., Ballentine, G., Attane, C., Iglesias, J., Poursharifi, P., Zhang, D., Nguyen, T.A., Erb, H., Prentki, R., et al. (2016). alpha/beta-Hydrolase Domain 6 Deletion Induces Adipose Browning and Prevents Obesity and Type 2 Diabetes. Cell Rep. *14*, 2872–2888. https://doi.org/10.1016/j.celrep.2016.02.076.

44. Zhou, P., Werner, J.H., Lee, D., Sheppard, A.D., Liangpunsakul, S., and Duffield, G.E. (2015). Dissociation between diurnal cycles in locomotor

activity, feeding behavior and hepatic PERIOD2 expression in chronic alcohol-fed mice. Alcohol *49*, 399–408. https://doi.org/10.1016/j.alcohol.2015.03.005.

45. Xu, H., Barnes, G.T., Yang, Q., Tan, G., Yang, D., Chou, C.J., Sole, J., Nichols, A., Ross, J.S., Tartaglia, L.A., and Chen, H. (2003). Chronic inflammation in fat plays a crucial role in the development of obesity-related insulin resistance. J. Clin. Invest. *112*, 1821–1830. https://doi.org/10.1172/JCI19451.
46. Apovian, C.M., Bigornia, S., Mott, M., Meyers, M.R., Ulloor, J., Gagua, M., McDonnell, M., Hess, D., Joseph, L., and Gokce, N. (2008). Adipose macrophage infiltration is associated with insulin resistance and vascular endothelial dysfunction in obese subjects. Arterioscler. Thromb. Vasc. Biol. *28*, 1654–1659. https://doi.org/10.1161/ATVBAHA.108.170316.
47. De Taeye, B.M., Novitskaya, T., McGuinness, O.P., Gleaves, L., Medda, M., Covington, J.W., and Vaughan, D.E. (2007). Macrophage TNF-alpha contributes to insulin resistance and hepatic steatosis in diet-induced obesity. Am. J. Physiol. Endocrinol. Metab. *293*, E713–E725. https://doi.org/10.1152/ajpendo.00194.2007.
48. Engin, A. (2017). The Pathogenesis of Obesity-Associated Adipose Tissue Inflammation. Adv. Exp. Med. Biol. *960*, 221–245. https://doi.org/10.1007/978-3-319-48382-5_9.
49. Surmi, B.K., and Hasty, A.H. (2008). Macrophage infiltration into adipose tissue: initiation, propagation and remodeling. Future Lipidol. *3*, 545–556. https://doi.org/10.2217/17460875.3.5.545.
50. Ni, Y., Ni, L., Zhuge, F., Xu, L., Fu, Z., and Ota, T. (2020). Adipose Tissue Macrophage Phenotypes and Characteristics: The Key to Insulin Resistance in Obesity and Metabolic Disorders. Obesity *28*, 225–234. https://doi.org/10.1002/oby.22674.
51. Murano, I., Barbatelli, G., Parisani, V., Latini, C., Muzzonigro, G., Castellucci, M., and Cinti, S. (2008). Dead adipocytes, detected as crown-like structures, are prevalent in visceral fat depots of genetically obese mice. J. Lipid Res. *49*, 1562–1568. https://doi.org/10.1194/jlr.M800019-JLR200.
52. Strissel, K.J., Stancheva, Z., Miyoshi, H., Perfield, J.W., 2nd, DeFuria, J., Jick, Z., Greenberg, A.S., and Obin, M.S. (2007). Adipocyte death, adipose tissue remodeling, and obesity complications. Diabetes *56*, 2910–2918. https://doi.org/10.2337/db07-0767.
53. Das, K., Lin, Y., Widen, E., Zhang, Y., and Scherer, P.E. (2001). Chromosomal localization, expression pattern, and promoter analysis of the mouse gene encoding adipocyte-specific secretory protein Acrp30. Biochem. Biophys. Res. Commun. *280*, 1120–1129. https://doi.org/10.1006/bbrc.2001.4217.
54. Wang, Q.A., Tao, C., Jiang, L., Shao, M., Ye, R., Zhu, Y., Gordillo, R., Ali, A., Lian, Y., Holland, W.L., et al. (2015). Distinct regulatory mechanisms governing embryonic versus adult adipocyte maturation. Nat. Cell Biol. *17*, 1099–1111. https://doi.org/10.1038/ncb3217.
55. Straub, L.G., and Scherer, P.E. (2019). Metabolic Messengers: Adiponectin. Nat. Metab. *1*, 334–339. https://doi.org/10.1038/s42255-019-0041-z.
56. Martinez-Perez, B., Ejarque, M., Gutierrez, C., Nuñez-Roa, C., Roche, K., Vila-Bedmar, R., Ballesteros, M., Redondo-Angulo, I., Planavila, A., Villarroya, F., et al. (2016). Angiopoietin-like protein 8 (ANGPTL8) in pregnancy: a brown adipose tissue-derived endocrine factor with a potential role in fetal growth. Transl. Res. *178*, 1–12. https://doi.org/10.1016/j.trsl.2016.06.012.
57. Izumi, R., Kusakabe, T., Noguchi, M., Iwakura, H., Tanaka, T., Miyazawa, T., Aotani, D., Hosoda, K., Kangawa, K., and Nakao, K. (2018). CRISPR/Cas9-mediated Angptl8 knockout suppresses plasma triglyceride concentrations and adiposity in rats. J. Lipid Res. *59*, 1575–1585. https://doi.org/10.1194/jlr.M082099.
58. Vatner, D.F., Goedeke, L., Camporez, J.P.G., Lyu, K., Nasiri, A.R., Zhang, D., Bhanot, S., Murray, S.F., Still, C.D., Gerhard, G.S., et al. (2018). Angptl8 antisense oligonucleotide improves adipose lipid metabolism and prevents diet-induced NAFLD and hepatic insulin resistance in rodents. Diabetologia *61*, 1435–1446. https://doi.org/10.1007/s00125-018-4579-1.
59. Zhang, Z., Wu, H., Dai, L., Yuan, Y., Zhu, Y., Ma, Z., Ruan, X., and Guo, X. (2020). ANGPTL8 enhances insulin sensitivity by directly activating insulin-mediated AKT phosphorylation. Gene *749*, 144707. https://doi.org/10.1016/j.gene.2020.144707.
60. Kahn, B.B. (2019). Adipose Tissue, Inter-Organ Communication, and the Path to Type 2 Diabetes: The 2016 Banting Medal for Scientific Achievement Lecture. Diabetes *68*, 3–14. https://doi.org/10.2337/dbi18-0035.
61. de Jonge, L., and Bray, G.A. (1997). The thermic effect of food and obesity: a critical review. Obes. Res. *5*, 622–631. https://doi.org/10.1002/j.1550-8528.1997.tb00584.x.
62. Yang, Y., Jiao, X., Li, L., Hu, C., Zhang, X., Pan, L., Yu, H., Li, J., Chen, D., Du, J., and Qin, Y. (2020). Increased Circulating Angiopoietin-Like Protein 8 Levels Are Associated with Thoracic Aortic Dissection and Higher Inflammatory Conditions. Cardiovasc. Drugs Ther. *34*, 65–77. https://doi.org/10.1007/s10557-019-06924-7.
63. Liao, Z., Wu, X., Song, Y., Luo, R., Yin, H., Zhan, S., Li, S., Wang, K., Zhang, Y., and Yang, C. (2019). Angiopoietin-like protein 8 expression and association with extracellular matrix metabolism and inflammation during intervertebral disc degeneration. J. Cell Mol. Med. *23*, 5737–5750. https://doi.org/10.1111/jcmm.14488.
64. Zhang, Z., Yuan, Y., Hu, L., Tang, J., Meng, Z., Dai, L., Gao, Y., Ma, S., Wang, X., Yuan, Y., et al. (2023). ANGPTL8 accelerates liver fibrosis mediated by HFD-induced inflammatory activity via LILRB2/ERK signaling pathways. J. Adv. Res. *47*, 41–56. https://doi.org/10.1016/j.jare.2022.08.006.
65. La Cava, A. (2017). Leptin in inflammation and autoimmunity. Cytokine *98*, 51–58. https://doi.org/10.1016/j.cyto.2016.10.011.
66. Ouchi, N., and Walsh, K. (2007). Adiponectin as an anti-inflammatory factor. Clin. Chim. Acta *380*, 24–30. https://doi.org/10.1016/j.cca.2007.01.026.
67. Kanda, H., Tateya, S., Tamori, Y., Kotani, K., Hiasa, K.i., Kitazawa, R., Kitazawa, S., Miyachi, H., Maeda, S., Egashira, K., and Kasuga, M. (2006). MCP-1 contributes to macrophage infiltration into adipose tissue, insulin resistance, and hepatic steatosis in obesity. J. Clin. Invest. *116*, 1494–1505. https://doi.org/10.1172/JCI26498.
68. Kamei, N., Tobe, K., Suzuki, R., Ohsugi, M., Watanabe, T., Kubota, N., Ohtsuka-Kowatari, N., Kumagai, K., Sakamoto, K., Kobayashi, M., et al. (2006). Overexpression of monocyte chemoattractant protein-1 in adipose tissues causes macrophage recruitment and insulin resistance. J. Biol. Chem. *281*, 26602–26614. https://doi.org/10.1074/jbc.M601284200.
69. Jialal, I., Kaur, H., and Devaraj, S. (2014). Toll-like receptor status in obesity and metabolic syndrome: a translational perspective. J. Clin. Endocrinol. Metab. *99*, 39–48. https://doi.org/10.1210/jc.2013-3092.
70. Kahn, C.R., Wang, G., and Lee, K.Y. (2019). Altered adipose tissue and adipocyte function in the pathogenesis of metabolic syndrome. J. Clin. Invest. *129*, 3990–4000. https://doi.org/10.1172/jci129187.
71. Santoro, A., and Kahn, B.B. (2023). Adipocyte Regulation of Insulin Sensitivity and the Risk of Type 2 Diabetes. N. Engl. J. Med. *388*, 2071–2085. https://doi.org/10.1056/NEJMra2216691.
72. Smith, U., and Kahn, B.B. (2016). Adipose tissue regulates insulin sensitivity: role of adipogenesis, de novo lipogenesis and novel lipids. J. Intern. Med. *280*, 465–475. https://doi.org/10.1111/joim.12540.
73. Zhang, R., and Zhang, K. (2024). A unified model for regulating lipoprotein lipase activity. Trends Endocrinol. Metab. *35*, 490–504. https://doi.org/10.1016/j.tem.2024.02.016.
74. Sassmann, A., Offermanns, S., and Wettschureck, N. (2010). Tamoxifen-inducible Cre-mediated recombination in adipocytes. Genesis *48*, 618–625. https://doi.org/10.1002/dvg.20665.
75. Yang, Y., Smith, D.L., Jr., Keating, K.D., Allison, D.B., and Nagy, T.R. (2014). Variations in body weight, food intake and body composition after long-term high-fat diet feeding in C57BL/6J mice. Obesity *22*, 2147–2155. https://doi.org/10.1002/oby.20811.

76. Jeffery, E., Church, C.D., Holtrup, B., Colman, L., and Rodeheffer, M.S. (2015). Rapid depot-specific activation of adipocyte precursor cells at the onset of obesity. Nat. Cell Biol. *17*, 376–385. https://doi.org/10.1038/ncb3122.

77. Matthews, D.R., Hosker, J.P., Rudenski, A.S., Naylor, B.A., Treacher, D.F., and Turner, R.C. (1985). Homeostasis model assessment: insulin resistance and beta-cell function from fasting plasma glucose and insulin concentrations in man. Diabetologia *28*, 412–419. https://doi.org/10.1007/BF00280883.

78. Pelletier, A., Joly, E., Prentki, M., and Coderre, L. (2005). Adenosine 5'-monophosphate-activated protein kinase and p38 mitogen-activated protein kinase participate in the stimulation of glucose uptake by dinitrophenol in adult cardiomyocytes. Endocrinology *146*, 2285–2294. https://doi.org/10.1210/en.2004-1565.

79. Attane, C., Daviaud, D., Dray, C., Dusaulcy, R., Masseboeuf, M., Prevot, D., Carpene, C., Castan-Laurell, I., and Valet, P. (2011). Apelin stimulates glucose uptake but not lipolysis in human adipose tissue ex vivo. J. Mol. Endocrinol. *46*, 21–28. https://doi.org/10.1677/JME-10-0105.

80. Ochoa-Sanchez, R., Oliveira, M.M., Tremblay, M., Petrazzo, G., Pant, A., Bosoi, C.R., Perreault, M., Querbes, W., Kurtz, C.B., and Rose, C.F. (2021). Genetically engineered E. coli Nissle attenuates hyperammonemia and prevents memory impairment in bile-duct ligated rats. Liver Int. *41*, 1020–1032. https://doi.org/10.1111/liv.14815.

81. Parlee, S.D., Lentz, S.I., Mori, H., and MacDougald, O.A. (2014). Quantifying size and number of adipocytes in adipose tissue. Methods Enzymol. *537*, 93–122. https://doi.org/10.1016/B978-0-12-411619-1.00006-9.

STAR★METHODS

KEY RESOURCES TABLE

REAGENT or RESOURCE	SOURCE	IDENTIFIER
Antibodies		
Angptl8	ThermoFisher	Cat# PA5-38043; RRID: RRID: AB_2554647
β-actin	Sigma-Aldrich	Cat#A5441; clone: AC-15; RRID: AB_476744
Mac-2	Biolegend	Cat# 125402; clone M3/38; RRID: AB_1134238; RRID: AB_1134237
Chemicals, Peptides, and Recombinant Proteins		
Tamoxifen	Sigma-Aldrich	Cat# T5448
High Fat Diet	Research Diet	Cat# D12451
D-Fructose	Bioshop	Cat# FRC180.5
Normal Diet, ND	Research Diet	Cat# D12450H
D-(+)-Glucose	BioShop	Cat# GLU601.5
Insulin	Eli Lilly	HumulinR
BCA	Thermofisher	Cat# 23225
NEFA	Fujiflim	HR Series NEFA-HR(2)
[3H]-2-deoxy-D-glucose	Perkin Elmer	Cat# NET.549
Critical Commercial Assays		
Mouse Total Adiponectin ELISA	ALPCO	Cat# 22-ADPMS-E01
Mouse Angiopoietin Like Protein 8 ELISA	Assay Genie	Cat# MODL00076
Lipoprotein Lipase (LPL) Activity Assay (Fluorometric)	Cell Biolabs	Cat# STA-610
Insulin	Perkin Elmer	Cat# AL204
Leptin	Perkin Elmer	Cat# AL225
Experimental Models: Organisms/Strains		
Mouse: Angptl8fl/fl: C57BL/6N	Ingenious Targeting Laboratory	N/A
Mouse: Adipoq-CreERT2: C57BL/6N	Sassmann, A, et al.[74]	N/A
Oligonucleotides		
BLUelf Prestained Protein Ladder	Froggabio, Concord, Canada	# PM008-0500
Genotyping primer: Angptl8-lox Forward: GCTTATCGGACCTCACTTGC Reverse: GTGCTTGTGTTTGGGCAC	This Paper	N/A
Genotyping primer: Adipoq-Cre Forward: TGGTGCATCTGAAGACACTACA Reverse: TGCTGTTGGATGGTCTTCACAG	Poursharifi, P, et al.[41]	N/A
For Primer list see Table S1	This paper	N/A
Software and Algorithms		
Fiji	https://fiji.sc/	N/A
Prism	Graphpad	v10.2.0

EXPERIMENTAL MODEL

Adipose-specific ANGPTL8 conditional KO mice and corresponding control mice (wildtype, Angptl8Flox/Flox and Adipoq-Cre mice), all on the C57BL6N genetic background were used in the study. All the mice were housed in individual cages and kept at 12-h light/dark cycle at 21°C with free access to water. We employed male mice at the age of 8 weeks when the first dose of tamoxifen was given. At this time, the mice were fed either normal chow diet or high fat/high fructose diet as detailed in the Methods section below. Male mice were used in this study as female mice are less responsive to diet induced obesity. All procedures for mouse studies were approved by the Institutional Committee for the Protection of Animals at the CRCHUM.

METHOD DETAILS

Generation of adipose-specific ANGPTL8 conditional KO mice and breeding strategy

Heterozygous ANGPTL8lox/+ mice where exons 1 to 4 of ANGPTL8 gene are flanked with *LoxP* sites were generated by Ingenious Targeting Laboratory (Ronkonkoma, NY). The donor targeting vector was designed to insert the *loxP* sequences on the 5′ side of exon 1 and at the 3′ end of the FRT-flanked *Neo* selection cassette (after exon 4) (Figure 1A). This targeting vector was then introduced into FLP C57BL/6 ES cells via electroporation. ES cell clones with successful targeting were microinjected into Balb/c blastocysts to create chimeras. Subsequent mating with wildtype (WT) C57BL/6N mice resulted in the generation of heterozygous ANGPTL8lox/+ mice. Breeding of these mice led to the production of homozygous ANGPTL8lox/lox (ANGPTL8flox/flox) mice.

Homozygous ANGPTL8lox/lox mice were bred with heterozygous Adipoq-CreERT2 mice, on a C57BL/6N background,[74] generating Adipoq-CreERT2, ANGPTL8lox/+ mice. This lineage was further subjected to a second round of breeding to obtain wildtype (WT), homozygous ANGPTL8lox/lox (Fl/Fl), Adipoq-Cre (Cre), and homozygous ANGPTL8lox/lox-Adipoq-Cre (to generate AT-A8–KO mice through tamoxifen (TMX) injection). At 8 weeks of age, male mice with genotypes Cre, and ANGPTL8lox/lox-Adipoq-Cre (KO) were administered TMX (80 mg/kg body weight, dissolved in 10% ethanol in corn oil; oral gavage) every other day for 3 times. Male mice were used in this study as female mice are less responsive to diet induced obesity.[75]

To assess the presence of the WT or floxed ANGPTL8 allele, DNA from ear punch tissue fragments was analyzed using the following primers: Forward: 5′- GCTTATCGGACCTCACTTGC -3’; Reverse 5′- GTGCTTGTGTTTGGGCAC -3′. The presence of Cre transgene was determined using the primers: Forward: 5′- TGGTGCATCTGAAGACACTACA -3′, Reverse: 5′- TGCTGTTGG ATGGTCTTCACAG -3’. Genomic PCR confirmed specific amplification of a 686 bp DNA fragment corresponding to the floxed-ANGPTL8 allele, a 569 bp fragment corresponding to the WT ANGPTL8 allele, and the presence of the Adipoq-CreERT2 transgene with a 600 bp DNA fragment (Figure 1B).

High-fat high-fructose diet-induced obesity

Following TMX administration at 8 weeks, the mice received either a high-fat/high-sucrose diet (D12451, Research Diets, New Brunswick, NJ, consisting of 20 kcal% protein, 35 kcal% carbohydrates, and 45 kcal% fat) supplemented with 30% D-fructose (FRC180.5, BioShop, Burlington, ON, Canada) in the drinking water to form the high-fat/high-fructose (HFHF) diet, which better resembles the western diet,[41] or a control diet (normal diet, ND; D12450H, Research Diets) for a period of 23 weeks. A second round of TMX gavages (80 mg/kg body weight) was given 3 times in a week after 9 weeks on HFHF diet. It has been demonstrated that in long-term high fat diet feeding experiments in mice, even though the initial TMX dosing ensures Cre-mediated gene deletion in the existing mature adipocytes, an additional TMX dosing is required during the feeding regimen to ensure gene deletion in the newly formed mature adipocytes due to elevated adipogenesis, during the course of feeding.[76] Each of the groups, namely Cre-ND, Cre-HFD, KO-ND, and KO-HFD, consisted of 9–10 male mice. Body mass, food and water intake were measured weekly. Mice were euthanized by ketamine/xylazine overdose intra-peritoneal injection, followed by cardiac puncture blood collection. Livers and adipose tissues were collected and weighed. Samples were either fixed in formalin for histological analysis or frozen in liquid nitrogen and stored at −80°C until further analyses.

Metabolic studies using Comprehensive Lab Animal Monitoring System (CLAMS)

Respiration, energy expenditure and locomotion of the AT-A8-KO and control Cre mice (after 21 weeks on normal or HFHF diet) were assessed by individually placing the mice in metabolic chambers (CLAMS, Columbus Instruments) for 72 h (24 h of adaptation at 22°C and measurements for the next 48 h at 22°C). Oxygen consumption (VO2), CO2 production (VCO2), respiratory exchange ratio (RER), locomotor activity, and energy expenditure were continuously monitored using indirect calorimetry. Energy expenditure was quantified as a function of metabolic mass, (lean mass +0.2 × fat mass).[43,44] Lean and fat mass were assessed using Magnetic Resonance (EchoMRI Analyzer-700).

Oral glucose tolerance test

An oral glucose tolerance test (OGTT) was conducted on KO or Cre mice after 20 weeks on either the HFHF or control diet.[41] Following a 6-h food withdrawal, glucose (2 g/kg body weight) was orally administered through gavage.

Tail vein blood samples were collected at 0, 15, 30, 60, and 120 min after glucose administration for the measurement of blood glycemia levels using a Contour glucometer (Ascensia Diabetes Care, Mississauga, ON, Canada), and for the analysis of total plasma insulin content.

Insulin tolerance test

An insulin tolerance test (ITT) was conducted following a 23-week on either the HFHF or control diet in KO and Cre mice. After a 4-h food withdrawal period, insulin (1 U/kg body weight, HumulinR; Eli Lilly, ON, Canada) was administered intraperitoneally. Blood samples were collected from the tail vein for glucose monitoring at 0, 15, 30, 45, 60, 90, and 120 min post-injection. HOMA-IR was calculated using the following formula ((fasting insulin (mU/L) * fasting glucose (mmol/L))/22.5).[77]

Glucose uptake assay

Brown adipose tissue (BAT), soleus, and collagenase-isolated mature adipocytes from visceral white adipose tissue (VAT) and subcutaneous white adipose tissue (SAT) of KO and Cre mice fed with HFHF were rinsed, weighed, and used for measurements of basal and insulin-stimulated glucose uptake using radioactive [3H]-2-deoxy-D-glucose (2-DG).[41,78,79] Briefly, the isolated adipocytes were preincubated 10 min in Krebs-Ringer bicarbonate HEPES buffer (KRBH), pH 7.4, containing BSA (2 mg/ml). The cells were then incubated for 45 min in the presence or absence of 100 nM insulin). The medium was then supplemented with 0.1 mM [3H]-2-DG (0.25 μCi/mL) for 10 min. At the end of the incubation, the adipocytes were washed twice with KRBH and then lysed using 500 μL NaOH (1M) at 50°C for 20 min, followed by neutralization with 500 μL HCl (1M). Cell-associated radioactivity was quantified by scintillation counting. Glucose uptake was normalized to total cellular protein content.

Plasma parameters

All the plasma parameters, except fasting glycemia, were measured under fed condition. Plasma lipid profiles from control and HFHF diet fed KO and Cre mice were assessed. Plasma cholesterol, low-density lipoprotein-cholesterol (LDL-C), high-density lipoprotein-cholesterol (HDL-C) and TG were measured using a Cobas C111 analyzer (Roche, Laval, QC, Canada).[80] Additionally, plasma insulin (AL204, PerkinElmer, Vaughan, ON, Canada), leptin (AL225, PerkinElmer), FFA (Fujifilm, Lexington, MA), adiponectin (22-ADPMS-E01, Alpco, Salem, NH), and inflammation markers (IL-6, TNFα, MCP-1) were quantified at the Metabolomic Core Facility of CRCHUM using EnVision (PerkinElmer). Plasma Angptl8 levels were measured using a commercially available ELISA kit (Assay Genie, Cat# MODL00076).

Tissue histology and analysis

Freshly isolated adipose tissues were fixed in 10% formalin, followed by dehydration and paraffin embedding before sectioning. Histological sections were stained with hematoxylin and eosin (H&E). Image analysis for cell size and number was performed using ImageJ Version 1.53k (National Institutes of Health, Bethesda, MD). The assessment of average area, frequency distribution, and adipocyte count in SAT and VAT was carried out.[81] In VAT, crown like structures (CLS) were counted from Mac-2 (Biolegend, 125402; clone M3/38, San Diego, CA) -stained slides and quantified. Immunohistochemistry was performed by the Molecular Pathology Core Facility of CRCHUM.

Immunoblotting

Collagenase-isolated mature adipocytes obtained from VAT and SAT of KO and Cre mice fed control or HFHF diet, were lysed with RIPA lysis buffer (20 mM Tris-HCl, pH 7.2, containing 150 mM NaCl, 1 mM EDTA, 1 mM EGTA, 1% v/v Triton X-100, 0.1% SDS, and protease inhibitors). After protein quantification by BCA (Thermo Fisher, Toronto, ON, Canada), 35 μg protein was used for western blot analysis with antibodies against ANGPTL8 (Thermo Fisher, PA5-38043) and β-actin (Sigma-Aldrich, A5441; clone: AC-15).

RNA extraction and quantitative PCR

Total RNA was isolated from tissues using the RNeasy Mini Kit (Qiagen). Following reverse transcription of 2 μg RNA to cDNA, gene expression was determined by quantitative PCR using SYBR Green (Applied Biosystems, Cat.# 4309155). Primers used were listed in the Table S1.

QUANTIFICATION AND STATISTICAL ANALYSIS

The results are presented as mean ± SEM. All data were analyzed using GraphPad Prism, version 10 Software. Statistical differences between 2 groups were assessed by unpaired, two-tailed Student's t test or multiple unpaired t-test for multiple comparison with Holm-Šídák correction and between multiple groups using one-way or two-way ANOVA with Bonferroni or Tukey's post hoc testing for multiple comparisons, as indicated. A p value of <0.05 was considered statistically significant.